

Electromagnetic excitation rates for nuclear isomers in a hot dense plasma

T.C. Luu, J.L. Friar, and A.C. Hayes

Theoretical Division, Los Alamos National Laboratory

MS-227 Los Alamos, NM 87545, USA

Correspondence: Thomas Luu

Los Alamos National Laboratory

T-6 Division, MS B227

Los Alamos, NM 87545

Phone: (505) 667-3612

Fax: (505) 664-0007

tluu@lanl.gov

18 total pages

3 tables

1 figure

arXiv:nucl-th/0412092v1 22 Dec 2004

Electromagnetic excitation rates for nuclear isomers in a hot dense plasma

T.C.Luu,* J.L. Friar, and A.C. Hayes

Theoretical Division, Los Alamos National Laboratory,

MS-227, Los Alamos, New Mexico 87545, USA

(Dated: July 17, 2018)

Abstract

In high neutron flux environments where isomers can be strongly populated by nucleonic reactions, isotope abundances from reaction network chains can be affected by the population of nuclear isomers. At high temperatures and densities there is the additional possibility of populating these isomers electromagnetically. Here we examine the rates for electromagnetic excitation of the isotopes of several isomers of interest both in astrophysics and applied physics (e.g. ^{235}U , ^{193}Ir , and $^{87,88}\text{Y}$). We consider six possible electromagnetic processes, namely, photo-absorption, inverse internal conversion, inelastic electron scattering, Coulomb excitation, (γ, γ') and $(e, e'\gamma)$ reactions. We find that for plasma temperatures $kT \sim 1 - 10$ keV the electromagnetic reactions rates are negligible. Thus, we conclude that reaction network calculations do not need to include for the possibility of electromagnetically exciting nuclear isomers. This is true in both stellar and terrestrial thermonuclear explosions, as well as in plasma conditions expected at the National Ignition Facility.

*tluu@lanl.gov

I. INTRODUCTION

In a hot dense plasma short-lived excited states of the nucleus with excitation energies on the order of the temperature of the plasma reach thermal equilibrium with the nuclear ground state and their relative population is determined by a Boltzmann distribution. Nucleosynthesis calculations usually try to take these states into account, though little is known about their nucleonic reaction properties (see, for example, Ref[1]). Recently there has been increased interest in the reaction properties of a certain set of nuclear excited states: nuclear spin isomers. These isomers are characterized by their relative long lifetimes due to their large angular momentum compared to their respective ground states. Particular interest has been concentrated on the 77 eV isomer of ^{235}U , where studies suggest that this isomer is populated strongly in the (n, n') reaction as well as in the $^{234}\text{U}(n, \gamma)$ reaction, and that the fission and neutron capture cross sections for this isomer are significantly different than that of the ^{235}U ground state[2, 3]. Thus, in high neutron flux environments, where two- or multi-neutron reactions are highly probable, reactions on this isomer can affect the reaction network chain involving the Uranium isotopes. The question we wish to address here is whether nuclear isomers can be populated by electromagnetic interactions as well. In a hot dense plasma environment there are several electromagnetic mechanisms to be considered at leading and sub-leading order in the fine structure constant α , namely: photo-absorption, inverse internal conversion, inelastic electron scattering, Coulomb excitation, (γ, γ') , and $(e, e'\gamma)$ [16]. Figure 1 shows the Feynman diagrams for these processes.

The electromagnetic excitation rates for all of these processes depend, of course, on the temperature kT of the plasma, the excitation energy E_m of the isomer, and the lifetime $\tau_{1/2}$ of the isomer. To simplify calculations, we assume that nuclei are completely stripped of their electrons in the plasma. Where possible, we give estimates to the errors of this assumption. We present expressions for these electromagnetic processes and examine the rates for certain nuclear isomers. Of particular interest for applied physics are the low-lying isomers of ^{235}U , ^{193}Ir , $^{87,88}\text{Y}$. Their properties, as well as those of other isomers considered in this paper, are listed in Table I. The half-lives of these isomers range from 0.3 msec to years and their excitation energies from ~ 77 eV - 2.5 MeV.

II. ELECTROMAGNETIC EXCITATION RATES

The total reaction width can be expressed as the sum of its constituent widths:

$$\Gamma_{total} = \Gamma_{\gamma} + \Gamma_{i.c.} + \Gamma_{i.e.s.} + \dots \quad (1)$$

Traditionally, this width is expressed as [4, 5]

$$\begin{aligned} \Gamma_{total} &= \Gamma_{\gamma} + \alpha_{i.c.}\Gamma_{\gamma} + \alpha_{i.e.s.}\Gamma_{\gamma} + \dots \\ &= \Gamma_{\gamma}(1 + \alpha_{i.c.} + \alpha_{i.e.s.} + \dots). \end{aligned} \quad (2)$$

Here *i.c.* refers to internal conversion, *i.e.s.* refers to inelastic electron scattering, and so forth. As can be seen from Eq. (2), calculation of a particular channel width Γ_i involves calculating both Γ_{γ} and α_i , where $\alpha_{\gamma} = 1$ for the case of photo-absorption. The reaction rate per nucleon for a particular channel *i* is given by

$$R_i = \int \sigma_i(E) d(\Phi(E)) \quad (3)$$

where $\Phi(E)$ is the flux of incoming particles responsible for that particular reaction and $\sigma_i(E)$ is the cross section. Due to the relatively long lifetimes of these isomers (*i.e.* $\Gamma_{total} \ll E_m$), the cross section is well approximated by

$$\sigma_i(E) \stackrel{\Gamma_{tot} \rightarrow 0}{\approx} \frac{2\pi^2}{k^2} \Gamma_i \delta(E - E_m), \quad (4)$$

where E_m is the excitation energy of the isomer and k is the wavenumber for the incoming particle.

A. Photo-absorption

We assume that in the system of interest the plasma has reached thermal equilibrium so that the photon flux is described by a Plankian distribution,

$$\begin{aligned} d(\Phi_{\gamma}(E)) &= \frac{c}{\pi^2(\hbar c)^3} \frac{E^2}{e^{E/kT} - 1} dE \\ &\equiv cN(E)dE, \end{aligned} \quad (5)$$

where $N(E)$ is the photon number density in the energy window between E and $E + dE$. The photo-absorption rate per unit atom is then

$$R_\gamma = c \int_0^\infty N(E) \sigma_\gamma(E) dE \quad (6)$$

$$\sim \frac{2}{e^{E_m/kT} - 1} \frac{\Gamma_\gamma}{\hbar}. \quad (7)$$

Here $\sigma_\gamma(E)$ is the photo-absorption cross section. Equation 7 follows from substituting Eq. 4 into Eq. 6. In the long-wavelength approximation (which is valid for the plasma conditions considered here) the width Γ_γ can be expressed in terms of reduced multipolarity transition probabilities $B(\pi\lambda)$,

$$\Gamma_\gamma(\pi\lambda : J_i \rightarrow J_f) = \frac{8\pi(\lambda + 1)}{\lambda[(2\lambda + 1)!!]^2} \left(\frac{E_m}{\hbar c}\right)^{2\lambda+1} B(\pi\lambda : J_i \rightarrow J_f) \quad (8)$$

In general, calculating $B(\pi\lambda)$ is very difficult because it depends on the initial- and final-state nuclear wavefunctions, which are not typically known. Naive estimates can be made if one invokes the extreme single-particle approximation, giving the well-documented *Weisskopf* expressions[5],

$$\begin{aligned} B(E\lambda : J_i \rightarrow J_f) &= \frac{1}{4\pi} \left(\frac{3}{3 + \lambda}\right)^2 R^{2\lambda} e^2 \text{fm}^{2\lambda} \\ B(M\lambda : J_i \rightarrow J_f) &= \frac{10}{\pi} \left(\frac{3}{3 + \lambda}\right)^2 R^{2\lambda-2} \mu_N^2 \text{fm}^{2\lambda-2}, \end{aligned} \quad (9)$$

where $R \sim 1.2 A^{1/3}$ and μ_N is the Bohr magneton. Near closed-shell nuclei, Weisskopf estimates give reasonable agreement with experimental values. However, for nuclei that exhibit strong collective degrees of freedom, the Weisskopf estimates are too small, sometimes by a few orders of magnitude[6].

Since the half-life of the isomer of ^{235}U is about 26 minutes, temperatures of ~ 150 keV would be required for the reaction rate per unit atom to reach a value of one-per-second. Thus, photo-absorption does not provide a significant mechanism for populating the 77 eV isomer of ^{235}U . As can be seen from Table III, the photo-absorption rates for all the isomers considered here are negligible. Even with more accurate Weisskopf values, the photo-absorption rates of these isomers at these temperatures would still be very small.

B. Inverse Internal Conversion

In inverse internal conversion an electron from the plasma is captured into a bound atomic orbital, thereby exciting the nucleus. The capture energy of the electron must match the excitation energy of the nuclear isomer. The reaction rate is determined by the overlap of the continuum electron wavefunction with the bound atomic electron wavefunction, weighted by the nuclear transition matrix element. Since we assume that nuclei are stripped of all their electrons, all atomic shells (*i.e.* K , L_I , L_{II} , M_I , etc) can participate in the internal conversion process, as long as the kinematics of the process are satisfied. However, since the conversion happens near the nucleus, s-waves states typically dominate the transition. In most cases the electron can capture into the $1s_{1/2}$ K -shell. For isomers with very low excitation energies the electron can be captured only into a higher orbit. For example, the 77 eV isomer of ^{235}U can capture electrons only into very high ($n \geq 39$) outer atomic orbits, whereas both ^{242}Am and ^{193}Ir can capture electrons only into orbits with $n \geq 2$.

To obtain naive estimates of $\alpha_{i.c.}$, we assume relativistic hydrogenic wavefunctions for the bound electron and treat the nucleus as a point particle. The internal conversion coefficients for the innermost atomic orbits are thus given by[7]

$$\begin{aligned}\alpha_{i.c.}(E\lambda; \kappa_o = -1) &= \frac{2\pi\alpha\omega_\gamma}{\lambda(\lambda+1)} \sum_{\kappa} (2j+1) \begin{pmatrix} \frac{1}{2} & j & \lambda \\ \frac{1}{2} & -\frac{1}{2} & 0 \end{pmatrix}^2 |R_{-1,\kappa}(E\lambda)|^2 \\ \alpha_{i.c.}(M\lambda; \kappa_o = -1) &= \frac{2\pi\alpha\omega_\gamma}{\lambda(\lambda+1)} \sum_{\kappa} (2j+1)(\kappa-1)^2 \begin{pmatrix} \frac{1}{2} & j & \lambda \\ \frac{1}{2} & -\frac{1}{2} & 0 \end{pmatrix}^2 |R_{-1,\kappa}(M\lambda)|^2,\end{aligned}\tag{10}$$

where $j = |\kappa| - 1/2$ and ω_γ is the photon wave number. For $M\lambda$ transitions, κ can take on values of $-\lambda$ or $\lambda + 1$, while for $E\lambda$ transitions, $\kappa = \lambda$ or $-(\lambda + 1)$. The functions $R_{\kappa_o,\kappa}$ are given by

$$\begin{aligned}R_{\kappa_o,\kappa}(E\lambda) &= (\kappa_o - \kappa)(R_3 + R_4) + \lambda(R_4 - R_3) + \lambda(R_1 + R_2) \\ R_{\kappa_o,\kappa}(M\lambda) &= R_5 + R_6,\end{aligned}\tag{11}$$

where

$$\begin{aligned}
R_1 &= \int_0^\infty dr u_\kappa(p_e r) U_{\kappa_o}(\lambda_e r) h_\lambda^{(1)}(\omega_\gamma r) \\
R_2 &= \int_0^\infty dr v_\kappa(p_e r) V_{\kappa_o}(\lambda_e r) h_\lambda^{(1)}(\omega_\gamma r) \\
R_3 &= \int_0^\infty dr v_\kappa(p_e r) U_{\kappa_o}(\lambda_e r) h_{\lambda-1}^{(1)}(\omega_\gamma r) \\
R_4 &= \int_0^\infty dr u_\kappa(p_e r) V_{\kappa_o}(\lambda_e r) h_{\lambda-1}^{(1)}(\omega_\gamma r) \\
R_5 &= \int_0^\infty dr v_\kappa(p_e r) U_{\kappa_o}(\lambda_e r) h_\lambda^{(1)}(\omega_\gamma r) \\
R_6 &= \int_0^\infty dr u_\kappa(p_e r) V_{\kappa_o}(\lambda_e r) h_\lambda^{(1)}(\omega_\gamma r).
\end{aligned} \tag{12}$$

Here U and V correspond to the large and small components of the relativistic radial wavefunction for the bound electron in a Coulombic field, while u and v are the corresponding analogues for the Coulomb-distorted continuum wavefunction, and h_λ is the spherical Hankel function of order λ . Closed analytic forms can be derived for these integrals and are given, for example, in Refs.[8, 9].

Internal conversion coefficients for the innermost s-wave reactions are given in Table II. It is interesting to note that though internal conversion is suppressed by an order α compared to photo-absorption, there can be instances where there are enhancements to the reaction rate. This is clearly evident in ^{193}Ir , ^{242}Am , and especially ^{235}U . This behavior, though not apparent from Eq. 10, comes from the observation that the coefficients scale roughly as[10]

$$\alpha_{i.c.} \sim \begin{cases} \left(\frac{1}{\omega_\gamma}\right)^{\lambda+5/2} & \text{for } E\lambda \\ \left(\frac{1}{\omega_\gamma}\right)^{\lambda+3/2} & \text{for } M\lambda \end{cases}$$

Since the excitation energies of these isomers are relatively small, this enhancement is not surprising.

In the systems of interest (*e.g.* ignited inertial confinement fusion (ICF) capsules, nuclear explosions, and stellar environments), the temperatures attainable by the plasma are typically not high enough for nuclei to be completely stripped of their electrons, so that not all atomic shells are accessible for inverse internal conversion. Screening effects arising from the partial stripping of these nuclei affect the isomer excitation reaction rates by as much as 50% or more[17]. Self-consistent Dirac-Hartree-Fock calculations[11] have been performed to obtain internal conversion coefficients on some of the isomers considered here.

These calculations include the full effects of screening since the nuclei are not considered stripped of their electrons. Finite-size effects of the nucleus are considered as well. Hence these calculations use more realistic electronic wavefunctions than the simplistic hydrogenic wavefunctions considered here. We list these results in Table II for comparison. In general, calculations can differ by an order of magnitude (or more), as is evident for the case of ^{89m}Y . Yet the overall trend in relative sizes is consistent between the two methods.

The density of electrons is given by

$$n_e = \frac{m_e^{3/2}}{\sqrt{2}\pi^2\hbar^3} \int dE \frac{\sqrt{E}}{e^{(E-\mu)/kT} + 1} \quad (13)$$

Since there is no simple closed expression for the integral above, the chemical potential μ and density must be numerically solved self-consistently. The flux Φ_e of electrons is simply

$$\begin{aligned} \Phi_e &= \frac{1}{(2\pi\hbar)^3 m_e} \int_{v_z > 0} dp^3 \frac{p \cos(\theta)}{e^{(E(p)-\mu)/kT} + 1} \\ &= \frac{m_e}{4\pi^2\hbar^3} \int dE \frac{E}{e^{(E-\mu)/kT} + 1} \end{aligned} \quad (14)$$

Hence the differential flux is

$$d(\Phi_e) = \frac{m_e}{4\pi^2\hbar^3} \frac{E}{e^{(E-\mu)/kT} + 1} dE \quad (15)$$

Using Eqs. 3-4 gives the rate for isomeric production via internal conversion as

$$\frac{\alpha_{i.c.}}{4} \frac{1}{E^{(E_m-\mu)/kT} + 1} \frac{\Gamma_\gamma}{\hbar}. \quad (16)$$

To obtain estimates, we take an average electron density of $n_e \sim 100N_A \text{ cm}^{-3}$, where N_A is Avogadro's number. This corresponds to a chemical potential of $\mu = -.00275 \text{ keV}$ ($-.0622 \text{ keV}$) at $kT = 1 \text{ keV}$ (10 keV). Rates are listed in Table III. Even with the more accurate internal conversion coefficients of Ref.[11], rates would still be negligible.

C. Inelastic electron scattering

Formally, there is little difference between the theory of inelastic electron scattering and internal conversion. Physically, the main difference is that the final state electron still belongs to the continuum, as opposed to the bound-state orbital characteristic of inverse internal conversion. If the point-nucleus approximation is made, calculations of 'inelastic

scattering coefficients' are identical to the case with internal conversion coefficients—one just replaces the bound state wavefunctions with Coulomb distorted continuum wavefunctions, *i.e.*

$$\begin{aligned}
R_1 &= \int_0^\infty dr u_\kappa(pr)u_{\kappa_o}(p_o r)h_\lambda^{(1)}(\omega_\gamma r) \\
R_2 &= \int_0^\infty dr v_\kappa(pr)v_{\kappa_o}(p_o r)h_\lambda^{(1)}(\omega_\gamma r) \\
R_3 &= \int_0^\infty dr v_\kappa(pr)u_{\kappa_o}(p_o r)h_{\lambda-1}^{(1)}(\omega_\gamma r) \\
R_4 &= \int_0^\infty dr u_\kappa(pr)v_{\kappa_o}(p_o r)h_{\lambda-1}^{(1)}(\omega_\gamma r) \\
R_5 &= \int_0^\infty dr v_\kappa(pr)u_{\kappa_o}(p_o r)h_\lambda^{(1)}(\omega_\gamma r) \\
R_6 &= \int_0^\infty dr u_\kappa(pr)v_{\kappa_o}(p_o r)h_\lambda^{(1)}(\omega_\gamma r).
\end{aligned} \tag{17}$$

The above integrals can be computed numerically and the coefficients calculated using Eq. 10. Note that since these calculations deal with initial- and final-state *continuum* wavefunctions, coefficients no longer have any dependence on principal quantum numbers n . Nor do they take on discrete values since they are now functions of the electron's initial energy E , which is continuous. Since we approximate the reaction rate as being strongly peaked at the isomer's excitation energy (*i.e.* Eq. 4), the reaction rate is simply

$$\frac{\alpha_{i.e.s.}(E_m)}{4} \frac{1}{E^{(E_m-\mu)/kT} + 1} \frac{\Gamma_\gamma}{\hbar}. \tag{18}$$

Lastly, we assume the outgoing electron to be in an s-wave state. Table II tabulates the inelastic scattering coefficients at each isomer's excitation energy E_m . Table III shows rates for this reaction channel using the same conditions for the electron flux as in the previous section.

D. Coulomb excitation via heavy-ion scattering

Isomeric excitation could also happen via heavy-ion Coulomb excitation. In this case, the kinetic energy of the ions is small compared to its rest mass. Hence the ions can be treated non-relativistically. Reaction rates for heavy-ion Coulomb excitations can be directly calculated using similar methods discussed in the previous sections. However, it is simpler

(and perhaps more enlightening) to consider the ‘adiabaticity’ parameter[6, 12]

$$\xi = \eta \frac{E_m}{E}, \quad (19)$$

where E is the incoming ion energy and η is the classical Sommerfeld number given by

$$\eta = \alpha Z_1 Z_2 \frac{c}{v}. \quad (20)$$

Here Z_1 and Z_2 are the charges of the two scattering ions. The parameter ξ is a measure of the ratio between the collision time and the nuclear period. The larger the value of ξ , the more adiabatic the process becomes. Under conditions where the reaction is highly adiabatic, excitation of the nucleus is unlikely due to the fact that the nucleus has time to equilibrate under the influence of the external Coulomb field. Assuming the ions are in thermal equilibrium, the energy E can be approximated by $\frac{3}{2}kT$. Considering like-ion scattering, *i.e.* $Z_1 = Z_2$, the range of temperatures considered in this paper give

$$10^3 < \xi < 10^7.$$

The cross section for heavy-ion scattering scales roughly as $\sigma \sim e^{-2\pi\xi}$ [12], which in turn gives a similar scaling for the reaction rate. This rate is extremely small for large ξ . It is interesting to note that the exponential suppression is primarily a property of the *repulsive* Coulomb field[12]. The Coulomb barrier of these ions is too strong at these plasma temperatures for any isomeric excitation. For an attractive field with $Z_1 = 1$ (as in inelastic electron scattering), this exponential behavior is not as pronounced.

E. $\mathbf{N}(\gamma, \gamma')\mathbf{N}^*$ and $\mathbf{N}(e, e'\gamma)\mathbf{N}^*$

Another possible excitation process is through excitation to some high lying state, followed by gamma decay to the isomer. Excitation can be done via all the processes mentioned above, and in particular through (γ, γ') and $(e, e'\gamma)$ reactions. If one assumes that the rate of decay to the isomer is fast compared to the excitation process, then the rate of producing the isomer is approximately equal to the rate of excitation to the high-lying state. At first glance, such a process might seem plausible, since many of these higher-lying states are connected to the ground state by transitions of low multipolarity ($\lambda < 3, 4$). Such probability transitions may be larger by an order of magnitude or so compared to the isomeric

transitions. However, the fluence of incoming particles with the necessary energy to allow excitation is exponentially suppressed. Hence the gain from going to a lower multipolarity transition is quickly lost due to the fact that these high-lying states have large excitation energies compared to the isomers.

For example, consider the case of $^{89}_{39}\text{Y}$. The isomer state is connected via M1 transition to the $7/2^+$ state at energy 2529.87 keV. The transition probability between these two states is large ($\tau_{1/2}=.08$ ps). The $7/2^+$ state can be connected to the ground state via an M3 transition. But since the energy of this high lying state is large compared to the isomer, the rate of populating this state is much smaller than for the rate of directly populating the isomer. This suppression is roughly

$$\frac{R_{7/2^+}}{R_{isomer}} \approx \frac{e^{-2530/kT}}{e^{-909/kT}} = e^{-1621/kT}.$$

Here kT is in units of keV and R_{isomer} is the rate for producing the isomer directly from the ground state (via M4 transition). For a plasma temperature of 1 keV/10 keV, this suppression factor is vanishingly small. Similar suppression factors are found for the other isomers considered in this paper. Hence we conclude that population of isomers via (γ, γ') or $(e, e'\gamma)$ excitation is extremely unlikely (as opposed to the case of neutron-induced excitations, for example).

III. CONCLUSION

Nuclear isomers have played an increasingly important role in both astrophysics and applied physics phenomena. Typically these isomers are assumed to be populated solely by strong nuclear reactions. However, if the temperatures of the environment in which the isomers exist are high enough, there is the possibility that they be populated electromagnetically as well. In this paper we addressed this latter issue for typical plasma temperatures found in mundane laboratories and astrophysical environments (*i.e.* $kT \sim 1$ to 10 KeV).

In Sect. II we gave expressions for the reaction rates of the following electromagnetic processes: photo-absorption, inverse internal conversion, inelastic electron scattering, and Coulomb excitation. In Sect. IIE we argued that rates for (γ, γ') and $(e, e'\gamma)$ excitation were negligible. We made the assumption that the nucleus was a point particle and was completely stripped of its electrons due to the plasma environment. Furthermore, we only

considered s-wave scattering since this is usually the dominant channel. We found that all these processes contributed negligibly to the overall reaction rates for populating the nuclear isomers listed in Table I. Table III summarizes our claims.

These small rates can also be understood from simple dimensional analysis. As an example, consider photo-absorption on the ground state of ^{235}U . Using Eqns. 7-9 as guides, naive dimensional analysis gives the reaction rate for producing Uranium isomers as

$$R_\gamma \sim \frac{kT}{\hbar\omega_\gamma} \alpha Q^{2l} \frac{\omega_\gamma}{\hbar}, \quad (21)$$

where in this case $l=3$ and $Q = \frac{\omega_\gamma R}{c} \sim 2.4 \times 10^{-6}$. The dimensionless parameter Q sets the scale of the transition. Similar expressions for internal conversion and electron scattering can be determined from dimensional analysis as well, though in these cases it is the electron's momentum that determines the size of Q and not the photon's momentum. In all of these cases, Q is very small. An exception would be Coulomb excitation. However, as already mentioned in Sect. IID, the Coulomb barrier is prohibitive at the temperatures considered here.

Clearly the assumption that the nucleus is completely stripped of electrons is not valid. Furthermore, the expressions given in Sect. II were made under the assumption that the fluence of incoming particles is in thermal equilibrium. This is most likely not true in applied physics applications. However, due to the extremely small rates listed in Table III, more sophisticated calculations that take these issues into consideration are not warranted. Hence the assumption that nuclear isomers are produced entirely via strong nuclear reactions for the range of temperatures considered in this paper is valid.

-
- [1] R.A. Ward and W.A. Fowler. Thermalization of long-lived nuclear isomeric states under stellar conditions. *Astrophys.J.*, 238:266–286, 1980.
- [2] L.A. Popeko, G.A. Petrov, E.F. Kochubei, and T.K. Zvezdkina. On spontaneously fissioning u^{236m} isomer excited when capturing thermal neutrons. *Yad.Fiz.*, 17:234–241, 1973.
- [3] V.I. Mostovoi and G.I. Ustroev. Measurement of the fission cross section of the ^{235}u isomer by thermal neutrons. *At.Energ.*, 57:241–242, 1984.
- [4] J.M. Blatt and V.F. Weisskopf. *Theoretical Nuclear Physics*. Dover Publications, New York, 1979.
- [5] A. deShalit and H. Feshbach. *Theoretical Nuclear Physics vol. 1*. John Wiley & Sons, Inc., New York, 1974.
- [6] S.S.M. Wong. *Introductory Nuclear Physics*. John Wiley & Sons, New York, 1998.
- [7] M.E. Rose. *Internal Conversion Coefficients*. North Holland, New York, 1958.
- [8] W.D. Hamilton, editor. *The Electromagnetic Interaction in Nuclear Spectroscopy*. North Holland, New York, 1975.
- [9] R.F. O’Connell and C.O. Carroll. Internal conversion coefficients. *Phys.Rev.*, B138:1043–1054, 1965.
- [10] K. Alder, A. Bohr, T. Huus, B. Mottelson, and A. Winther. Study of nuclear structure by electromagnetic excitation with accelerated ions. *Rev.Mod.Phys.*, 28:432, 1956.
- [11] I.M. Band and M.B.A. Trzhaskovskaya. Internal conversion coefficients for low-energy nuclear transitions. *Atom.Dat. and Nuc.Dat.Tabs.*, 55:43, 1993.
- [12] L.C. Biedenharn and P.J. Brussaard. *Coulomb Excitation*. Clarendon Press, Oxford, 1965.
- [13] A. Veres. *Photoactivation of Isomers of Stable Nuclei and Recent Applications*. Akademiai Kiado, Budapest, 2002.
- [14] M. Morita. Nuclear excitation by electron transition and its application to uranium 235 separation. *Prog.Theor.Phys.*, 49:1574–86, 1973.
- [15] G. Claverie et al. Search for nuclear excitation by electronic transition in u-235. *Phys. Rev.*, C70:044303, 2004.
- [16] An omitted reaction at leading order in α is *inverse* internal pair-production. The threshold for this reaction occurs at $E > 1$ MeV (twice the electron mass), where E is the excitation

energy of the isomer. However, for the isomers considered here, this condition is not met. See Ref.[13] for descriptions of higher order processes.

- [17] If the nucleus is not completely stripped, reaction methods can also proceed via NEET[14, 15] (Nuclear Excitation by Electronic Transition). However, this method is even higher order in α , and for most of the isomers considered here, their excitation energies prohibit this excitation channel.

TABLE I: Nuclear isomers and their properties.

Nucleus	ground state (J^π)	multipole	isomer (J^π)	excitation energy E_m	$\tau_{1/2}$
^{87}Y	$1/2^-$	M4	$9/2^+$	380.7 keV	13.37 hr
^{88}Y	4^-	E3	1^+	392.9 keV	0.3 ms
^{88}Y	4^-	M4	8^+	674.6 keV	13.9 ms
^{89}Y	$1/2^-$	M4	$9/2^+$	909 keV	16.06 s
^{178}Hf	0^+	M8	8^-	1.174 MeV	4 s
^{178}Hf	0^+	E16	16^+	2.446 MeV	31 yr
^{193}Ir	$3/2^+$	M4	$11/2^-$	80.2 keV	10.53 d
^{235}U	$7/2^-$	E3	$1/2^+$	77 eV	26 min
^{242}Am	1^-	E4	5^-	48.63 keV	141 yr

TABLE II: Internal conversion and inelastic scattering coefficients. The second column gives the orbital in which the electrons are captured during inverse internal reactions. The third column lists the conversion coefficients calculated from relativistic hydrogenic wavefunctions, (*i.e.* Eqs. 10-12). The fourth column gives conversion coefficients derived from Dirac-Hartree-Fock calculations. The last column gives scattering coefficients for s-wave electrons calculated at the isomer's excitation energy E_m .

Isomer	final electron state	$\alpha_{i.c.}$ (r.h.wfs)	$\alpha_{i.c.}$ (D.H.F.) ^a	$\alpha_{i.e.s.}(E_m)$
^{87m}Y	$1s_{1/2}$.227		3.54
^{88m1}Y	$1s_{1/2}$.0245		1.48
^{88m2}Y	$1s_{1/2}$.0226		.323
^{89m}Y	$1s_{1/2}$.0078	.0819	.107
$^{178m1}\text{Hf}$	$1s_{1/2}$.342		3.05
$^{178m2}\text{Hf}$	$1s_{1/2}$.109		20.47
^{193m}Ir	$2s_{1/2}$	3641	2610	1.9E5
^{235m}U	$39s_{1/2}$	1.5E17	2.62E17 ^b	1.9E22
^{242m}Am	$2s_{1/2}$	3724		4.5E5

^aRef.[11]

^b O_{VI} shell result

TABLE III: Order of magnitude rates for electromagnetic reactions involving photoabsorption (P.A.), inverse internal conversion (I.I.C.), inelastic electron scattering (I.E.S.), and Coulomb excitation (C.E.). Rates are in units of inverse seconds, and come in pairs. The first number corresponds to the rate at $kT = 1$ keV, while the second to $kT = 10$ keV. We do not list rates for (γ, γ') and $(e, e'\gamma)$ since these are vanishingly small as well (see discussion in Sect. II E) .

Isomer	P.A.	I.I.C.	I.E.S.	C.E.
$87m\text{Y}$	$10^{-171} 10^{-22}$	$10^{-173} 10^{-26}$	$10^{-172} 10^{-25}$	$\sim e^{-10^7} e^{-10^6}$
$88m1\text{Y}$	$10^{-168} 10^{-14}$	$10^{-172} 10^{-20}$	$10^{-170} 10^{-18}$	$\sim e^{-10^7} e^{-10^5}$
$88m2\text{Y}$	$10^{-296} 10^{-32}$	$10^{-300} 10^{-38}$	$10^{-299} 10^{-37}$	$\sim e^{-10^7} e^{-10^6}$
$89m\text{Y}$	$10^{-397} 10^{-41}$	$10^{-401} 10^{-47}$	$10^{-399} 10^{-46}$	$\sim e^{-10^7} e^{-10^6}$
$178m1\text{Hf}$	$10^{-505} 10^{-70}$	$10^{-522} 10^{-75}$	$10^{-521} 10^{-74}$	$\sim e^{-10^8} e^{-10^7}$
$178m2\text{Hf}$	$10^{-1116} 10^{-160}$	$10^{-1119} 10^{-165}$	$10^{-1118} 10^{-164}$	$\sim e^{-10^7} e^{-10^6}$
$193m\text{Ir}$	$10^{-46} 10^{-14}$	$10^{-44} 10^{-14}$	$10^{-42} 10^{-12}$	$\sim e^{-10^7} e^{-10^6}$
$235m\text{U}$	$10^{-21} 10^{-20}$	$10^{-9} 10^{-7}$	$10^{-4} 10^{-2}$	$\sim e^{-10^4} e^{-10^3}$
$242m\text{Am}$	$10^{-31} 10^{-12}$	$10^{-30} 10^{-12}$	$10^{-28} 10^{-10}$	$\sim e^{-10^7} e^{-10^6}$

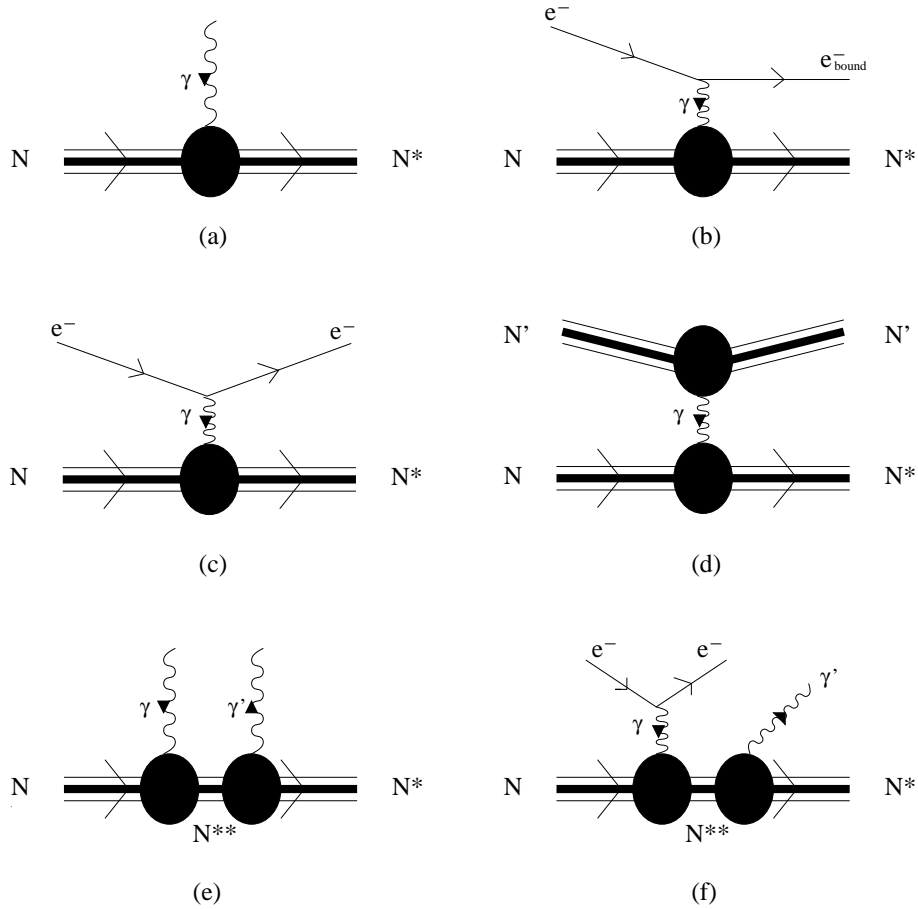


FIG. 1: Feynman diagrams representing the electromagnetic processes considered in this paper. Plot (a) represents photo-excitation. (b) represents inverse internal conversion, where the final electron is bound. (c) shows electron scattering, where the final electron belongs to the continuum. (d) shows ion-excitation, where N' is another ion. (e) shows (γ, γ') excitation. Finally, (f) shows $(e, e' \gamma)$ excitation.